

# Comparison of atmospheric pressure argon producing $O(^1S)$ and helium plasma jet on methylene blue degradation

Cite as: AIP Advances **11**, 045311 (2021); <https://doi.org/10.1063/5.0046948>

Submitted: 19 March 2021 • Accepted: 26 March 2021 • Published Online: 07 April 2021

 S. Jaiswal and  E. M. Aguirre



View Online



Export Citation



CrossMark

## ARTICLES YOU MAY BE INTERESTED IN

[Perspectives on cold atmospheric plasma \(CAP\) applications in medicine](#)

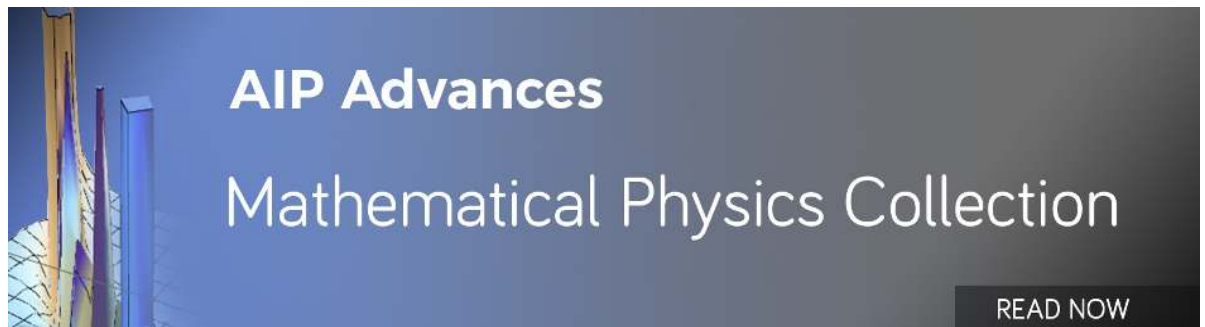
Physics of Plasmas **27**, 070601 (2020); <https://doi.org/10.1063/5.0008093>

[Plasma-based water purification: Challenges and prospects for the future](#)

Physics of Plasmas **24**, 055501 (2017); <https://doi.org/10.1063/1.4977921>

[Atmospheric pressure plasma jet in Ar and Ar/H<sub>2</sub>O mixtures: Optical emission spectroscopy and temperature measurements](#)

Physics of Plasmas **17**, 063504 (2010); <https://doi.org/10.1063/1.3439685>



AIP Advances  
Mathematical Physics Collection

READ NOW

# Comparison of atmospheric pressure argon producing O(<sup>1</sup>S) and helium plasma jet on methylene blue degradation

Cite as: AIP Advances 11, 045311 (2021); doi: 10.1063/5.0046948

Submitted: 19 March 2021 • Accepted: 26 March 2021 •

Published Online: 7 April 2021



View Online



Export Citation



CrossMark

S. Jaiswal<sup>1,2,a)</sup>  and E. M. Aguirre<sup>2</sup> 

## AFFILIATIONS

<sup>1</sup>Department of Chemical and Biological Engineering, Princeton University, Princeton, New Jersey 08544, USA

<sup>2</sup>Department of Physics, Auburn University, Auburn, Alabama 36832, USA

<sup>a)</sup>Author to whom correspondence should be addressed: [surabhjaiswal73@gmail.com](mailto:surabhjaiswal73@gmail.com)

## ABSTRACT

A solution of methylene blue dye was degraded under an atmospheric pressure plasma jet operating in a linear field configuration with pure argon or pure helium as working gases. Optical emission spectroscopy was carried out to understand the reactive species present with and without dye treatment. Both plasma jets contain reactive species such as OH, N<sub>2</sub>, and atomic oxygen (O). However, atomic oxygen takes a greatly different form depending on the working gas. In the argon plasma jet, we observe that most of the atomic oxygen produced is the O(<sup>1</sup>S)–O(<sup>1</sup>D) transition that also leads to the green colored plasma plume. On the other hand, the helium plasma jet produces the well known triplet states of oxygen at 777 and 844 nm. The absorption spectra confirmed the faster and more energy efficient degradation of the methylene blue dye when treated by the argon plasma jet. Argon plasma with enhanced atomic oxygen content can be utilized as a cheaper and efficient method for waste water treatment.

© 2021 Author(s). All article content, except where otherwise noted, is licensed under a Creative Commons Attribution (CC BY) license (<http://creativecommons.org/licenses/by/4.0/>). <https://doi.org/10.1063/5.0046948>

## I. INTRODUCTION

Atmospheric pressure plasma jets (APPJs) have been widely utilized in the last couple of decades due to their various applications in technology and biomedicine.<sup>1–3</sup> One interesting application of atmospheric pressure plasmas that has attracted research attention is the wastewater treatment of organic dyes. Given their stability and toxicity, these compounds are not easily broken down using traditional methods. Organic dyes from textile mills are found in waste water throughout the world where the total dye pollution is around  $1 \times 10^6$  kg per year.<sup>4,5</sup> Various chemical and biological methods have been used for organic dye degradation, but they are very expensive and produce excessive disposal (i.e., electrochemical or membrane filtration).<sup>6</sup> Adsorption is the generally preferred method given its ease of use, effectiveness, and recycling capability.<sup>7,8</sup> Regardless, additional techniques that are chemical-free and cost-effective have been an emerging area of research in recent years.

A relatively recent alternative to dye decomposition relevant to a range of dyes including methylene blue (MB) is plasma assisted

treatment.<sup>9</sup> Corona discharges<sup>10,11</sup> and plasma bubble systems<sup>12,13</sup> have been investigated with regard to MB degradation. The latter have some additional complexity, given the complex experimental hardware compared to freely flowing plasma jets. The noninvasive effect of plasma jets and the easy handling and negligible creation of reactive by-products make them attractive for MB degradation.<sup>14,15</sup> Moreover, the direct interaction with the atmosphere facilitates the formation of various reactive species responsible for MB degradation. Species that have been reported to contribute to MB degradation are hydrogen peroxide (H<sub>2</sub>O<sub>2</sub>), ozone (O<sub>3</sub>), and hydroxyl radicals (OH).<sup>16</sup> The OH radical was reported to be critically important for MB degradation.<sup>15</sup> Other reactive species such as atomic oxygen and excited argon<sup>14</sup> present in plasma jets in high density might be useful for MB degradation and require more research. The form of reactive species is governed by the carrier gas, whereas their concentrations are determined by the parameters such as gas flow rate and applied power.<sup>3,17–19</sup>

In this paper, we present a comparison of MB degradation with regard to the working gas (i.e., reactive species) in a linear electrode kilohertz APPJ. We use either pure helium or pure argon for creation

of a stable plasma jet while keeping all other parameters constant. The uniqueness of the argon plasma jet is the existence of the  $O(^1S)$  state, which is rarely observed in atmospheric plasmas.<sup>20</sup> Since  $O(^1S)$  has been declared highly effective for sterilization<sup>21</sup> and cleaning,<sup>22</sup> it seems plausible that its use would extend to other atmospheric plasma applications.

## II. EXPERIMENTAL SETUP

Figure 1(a) presents the photograph of the electrode arrangement of the plasma jet system. The detailed description of the experimental setup and diagnostics is reported elsewhere.<sup>20</sup> The experimental setup was used in the linear field configuration at a discharge voltage  $V_d = 10.2$  kV, frequency  $f = 21$  kHz, and gas flow rate of  $Q = 6$  sl/min. Figures 1(b) and 1(c) display the digital photographs

of the plasma jets of argon and helium, both generated by using the parameters mentioned above. It is important to mention that in our setup, the helium plasma can be excited at a lower applied voltage of 3 kV, whereas in the case of argon, the minimum applied voltage for plasma generation is 8 kV. Nevertheless, we use the same set of discharge parameters for a better comparison of these plasma jets and their effect on MB degradation.

The methylene blue solution was prepared by mixing 1 ml of 1% methylene blue dye and 149 ml of water. The solution was placed below the plasma jet with the plasma/liquid interface at  $z = -6$  mm.

## III. RESULTS AND DISCUSSION

A high voltage electric probe (Tektronix P6015A) and a Pearson current monitor probe (model 2877) are used to measure the

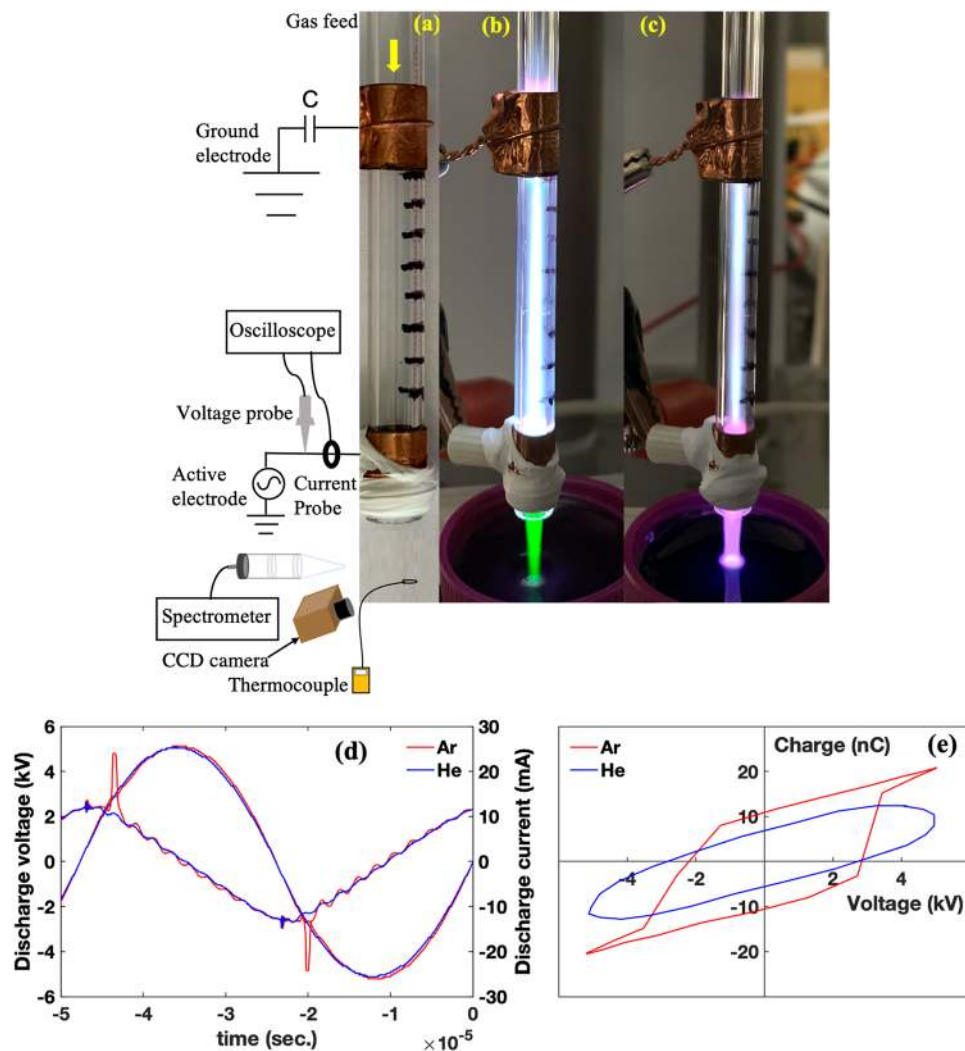


**FIG. 1.** (a) Photo of the electrode setup. A typical photograph of the (b) argon and (c) helium APPJ formed at  $f = 21$  kHz,  $V_d = 10.2$  kV, and a gas flow rate of  $Q = 6$  sl/min. (d) Current and voltage profiles of argon (red) and helium (blue). (e) The Lissajous plot showing the voltage–charge variation for argon (red) and helium (blue).

voltage and current waveforms, respectively. Figure 1(d) shows the current and the voltage waveform of the APPJs in helium and argon. The discharge current amplitude in both plasmas was almost the same. However, the current waveform of argon shows discharge peaks in both positive and negative sides and a number of distortions, whereas no discharge peak was seen in the current waveform of the helium plasma jet. The variation in discharge electrical characteristics for helium and argon plasma jets has been studied by the Lissajous voltage–charge plots,<sup>23</sup> which was estimated using a capacitance  $C$  of 1000 pF. An example of  $V/C$  plots for a fixed voltage of 10.2 kV is shown in Fig. 1(e), where the area under the curve corresponds to dissipative power over one cycle. The consumed power for the argon plasma jet is slightly higher (2.59 W) than the helium plasma jet (2.25 W).

The plasma jets were further characterized by determining the electron density ( $n_e$ ) by performing optical emission spectroscopy (OES) using a high resolution ( $\leq 0.05$  nm) spectrometer (Princeton Instruments SpectraPro<sup>®</sup> HRS-500). The electron number density ( $n_e$ ) is calculated using Stark broadening of the  $H_\beta$  line at 486.27 nm.<sup>24,25</sup> We only observe the  $H_\beta$  line for the helium plasma jet, so we are unable to use this method for calculating the density of the argon plasma jet. We follow the standard method as outlined by others, where the  $H_\beta$  spectrum is fitted with a Voigt profile, and the individual broadening mechanisms are determined. Table I lists the value of various broadening mechanisms, and the electron density is determined by<sup>26</sup>

$$n_e = \left( \frac{\Delta\lambda_S}{2 \cdot 10^{-11}} \right)^{3/2}. \quad (1)$$

The electron density of the helium plasma jet is  $1.4 \cdot 10^{14} \text{ cm}^{-3}$ , which agrees well with other helium plasma jets.<sup>27</sup> When dye treatment is occurring, the electron density drops to  $4.2 \cdot 10^{13} \text{ cm}^{-3}$ , which is close to the value where the Stark broadening method used here is not appropriate.

There are many factors that could influence MB degradation, but the primary factor is the chemical makeup of reactive species present in the plasma. The reactive species observed in the typical helium and argon spectra of the plasma jet are shown in Figs. 2 and 3, respectively. The helium and argon spectra contain most of the same signatures such as the OH band at 308–312 nm, excited nitrogen ( $N_2$  second positive system), and atomic oxygen at 777 and 844 nm. Excited helium neutral lines include 501.6 (metastable), 587.6, 667.8, 706.4, and 728.1 nm, but the metastable is much less intense. These lines indicate the presence of high energy electrons. The argon spectra are visibly dominated by the  $O(^1S)$  emission. Since argon neutral lines are highly intense as compared to species such as OH

TABLE I. Broadening mechanisms and values for the helium plasma jet.

Broadening	$\lambda$ (nm)
Natural <sup>28</sup>	$6.27 \cdot 10^{-5}$
Doppler <sup>28</sup>	0.006
Stark <sup>29</sup> MB	0.0538
Stark <sup>29</sup> no MB	0.0237
van der Waals <sup>30</sup>	0.0291
Instrumental	0.035

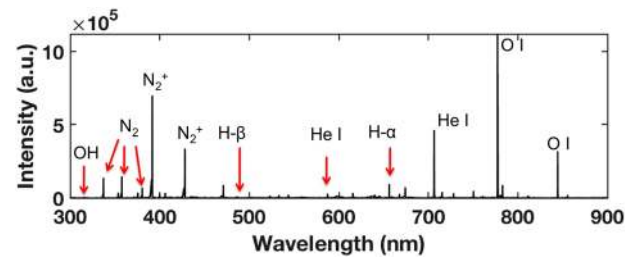


FIG. 2. Helium emission spectra of the plasma jet at  $z = -5$  mm.

and  $N_2$ , the spectra are shown in two windows for better visibility. A number of Ar I lines are observed in the range 415–430 nm. Most of these lines are from the same metastables as seen from the higher wavelengths but with far lower transition probabilities.<sup>31</sup> Although showing the same signature, the relative concentration of the reactive species in both the plasmas is very different. The formation of OH in the helium plasma is comparatively larger than that in the argon plasma, which is a key factor of MB decomposition. Atomic oxygen observed at 777 and 844 nm, which are both triplet states, is stronger in the helium plasma jet than in the argon plasma jet. However, argon plasma contains more atomic oxygen at 557.7 nm, which is due to  $O(^1S)$ – $O(^1D)$  transition. An increase in excited argon was also directly attributed to faster degradation of methylene blue in a microwave atmospheric pressure plasma jet.<sup>14</sup> We understand that the same situation is happening in our case due to high abundance of excited argon.

Atomic hydrogen lines are observed only in the helium plasma jet at 656 nm ( $H_\alpha$ ) and, on close inspection, 486 nm ( $H_\beta$ ). The hydrogen  $H_\alpha$  line originates due to the excitation of hydrogen atoms generated mostly by the dissociation of OH radicals because the  $H_\alpha$  emission intensity is stronger than that of OH.<sup>32</sup> Hydrogen is also formed from water in air (which is assumed at a constant concentration during the experiment), not by electron impact but from excited

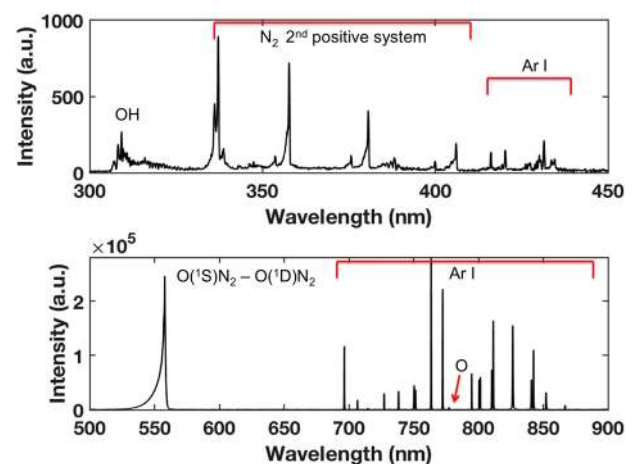


FIG. 3. Argon emission spectra of the plasma jet at  $z = -5$  mm.

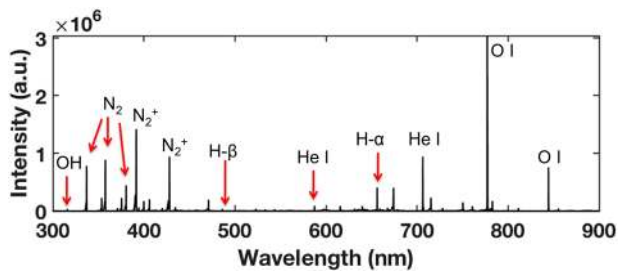


FIG. 4. Helium emission spectra of the plasma jet at  $z = -5$  mm during methylene blue dye treatment.

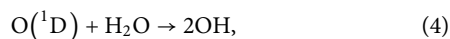
nitrogen,<sup>10</sup> according to



We observe no hydrogen, even under longer time integration, in the argon plasma jet, so the reaction to produce OH is notably different. Given the abundance of  $\text{O}(^1\text{S})$  and  $\text{O}(^1\text{D})$ , the most probable reactions for OH production in the argon plasma jet are



and



with reaction rates  $k = 3 \cdot 10^{-11}$  and  $k = 2.1 \cdot 10^{-10} \text{ cm}^3 \text{ s}^{-1}$ , respectively.<sup>33</sup> Since  $\text{O}_2$  and  $\text{N}_2$  quench the oxygen metastable states much faster than they decay by radiation, the latter OH production route with  $\text{O}(^1\text{D})$  is probably less significant.

The corresponding spectra of helium and argon plasma jets during dye treatment are presented in Figs. 4 and 5. The nature of the spectra remains similar for both plasmas; however, the relative intensity of various lines changed. The increase in the intensities of  $\text{H}_\alpha$ ,  $\text{H}_\beta$ , and OH, as shown in Fig. 4, signifies that the

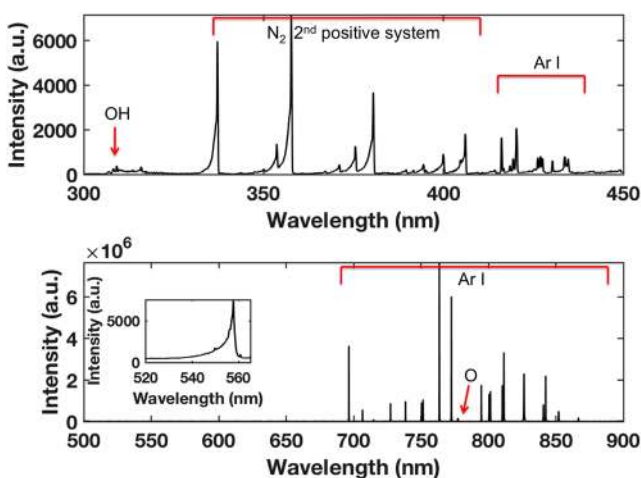
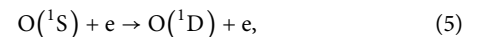


FIG. 5. Argon emission spectra of the plasma jet at  $z = -5$  mm during methylene blue dye treatment.

interaction of the plasma jet with water (the main content of our solution by weight and volume) provides the observed increase. The 557.7 nm, which corresponds to  $\text{O}(^1\text{S})$ , drops significantly relative to nitrogen molecular lines, as shown in Fig. 5. Since the  $\text{O}(^1\text{S})$  state is highly quenched by  $\text{N}_2$ , it is reasonable to conclude that the excited nitrogen concentration increased during dye treatment.

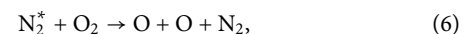
The visual effect of argon and helium plasma treatment on the MB solution is shown in Figs. 6(a) and 6(c). The degradation using helium appears very gradual, whereas it is very abrupt, after 5 min, using argon. The reactive species (OH,  $\text{H}_\alpha$ , and O) in the plasma plume interact with the aqueous solution and generate other reactive species that degrade methylene blue.<sup>34,35</sup> The OH radicals in the MB aqueous solution chemically react with the bonds of methylene blue, which causes decomposition.<sup>36</sup>

Even though the operating parameters for both plasma jets are the same, the discharge characteristics are different.<sup>37</sup> The measured spectra provide an estimation of the electron energy distribution function (EEDF) in the plasma. The EEDF is important for understanding the difference in reactive species production between the two plasma jets. The intensities of helium neutral lines are relatively weaker than those of  $\text{N}_2$  and oxygen, as shown in Fig. 2, due to the high excited energy of helium ( $>20$  eV), while those of  $\text{N}_2$  and O I lines are under 12 eV.<sup>15</sup> The ionization energies of nitrogen, argon, and helium are 15.5, 15.76, and 24.59 eV, respectively. Since we do not see any evidence of argon ions or even atomic nitrogen in Fig. 3, there are unlikely to be electrons with energies  $16 > E > 12$ , which would be responsible for excitation of argon and nitrogen. The energy of the excited argon metastable states, which are highly prevalent, is at least 11.55 eV. This energy is also inadequate to explain the existence of  $\text{N}_2^+$ . Overall, there is a lack of helium neutral lines compared to argon primarily because of the high excitation energy of helium ( $\sim 20$  eV) as compared to argon ( $\sim 12$  eV). The density (i.e., number) of electrons in the plasma that have high energy ( $>15$  eV) is orders of magnitude lower than the number of low energy ( $<5$  eV) electrons. Previous modeling has demonstrated that the helium plasma jet has a high energy tail and the argon plasma jet has a greater number of low energy electrons (below 5 eV).<sup>38</sup> The electron density was higher in the argon plasma jet as well. The  $\text{O}(^1\text{S})$  is a low energy level state that is excited via electron impact,

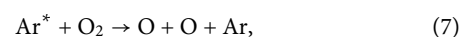


with a 4.19 eV electron. The other states of oxygen in the spectra [ $\text{O}(3p^3\text{P}) J = 1, 2, 3$ , 844 nm, and 10.99 eV] and [ $\text{O}(3p^5\text{P}) J = 1, 2, 3$ , 777 nm, and 10.74 eV] require higher energy electrons, which are present in higher density for the helium plasma jet.

The dissociation of oxygen differs significantly depending on the working gas. The helium plasma jet dissociates  $\text{O}_2$  via Penning ionization,



which we infer because of the large intensity of excited  $\text{N}_2$  in the helium plasma jet. Argon has less capability of producing Penning ionization.<sup>37</sup> The atomic oxygen in the argon plasma jet has been described before<sup>20</sup> and occurs via metastable reactions,





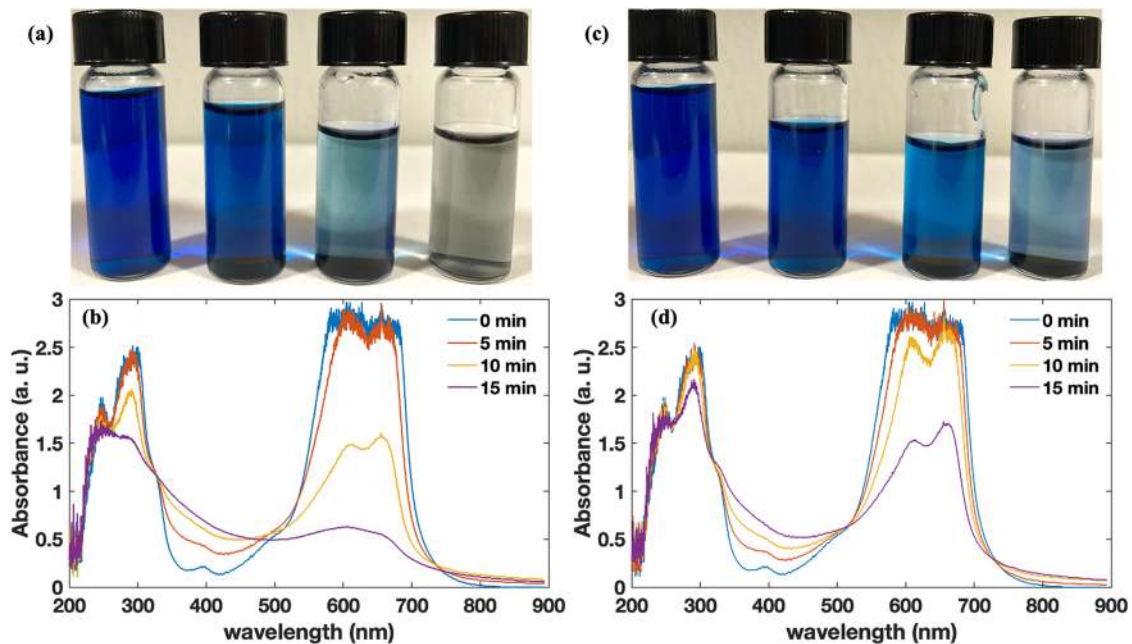
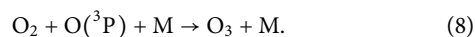


FIG. 6. Visual photographs of the degradation of (a) argon and (c) helium along with absorption of the dye for (b) argon and (d) helium.

which leads to the  $O(^1S)$  state with high density. Since the fraction of oxygen atoms that are in the  $O(^1S)$  state depends on  $n_e$ ,<sup>39</sup> it is likely that  $n_e$  is higher in the argon plasma jet, but only slightly.

The key result here is that the argon plasma jet degraded the dye faster and more efficiently. The main oxidative species in the plasma responsible for MB degradation are O, OH,  $H_2O_2$ , and  $O_3$ , and it is difficult to disentangle the effects of each species. Ozone ( $O_3$ ) is considered an extremely important oxidizer for degrading methylene blue<sup>10</sup> but is not generated in high concentrations for any atmospheric plasma process. Ozone is highly suppressed in air due to the reactions of oxygen and nitrogen.<sup>40,41</sup> Ozone is sometimes used as a proxy for atomic oxygen because the dominant reaction to create ozone is



It is quite common for ozone to be generated on purpose so that the concentration reached a meaningful amount.<sup>12</sup> Otherwise, in argon plasma jets, ozone is only 10–50 ppm. Ozone concentrations of >5000 ppm or ozone generators with gas bubbling systems degrade dyes much faster.<sup>42,43</sup> Our ozone concentration is likely low such that the more important species is atomic oxygen. There is certainly some oxygen in the ground state,  $O(^3P)$ , but we have not observed the relaxation to the ground state from  $O(^1S)$  at 295.9 nm or  $O(^1D)$  at 630.2 nm because of the long metastable lifetime—0.8 and 110 s, respectively.<sup>44,45</sup> Therefore, there would be little atomic oxygen necessary for the reaction to produce ozone. Even if the ground state oxygen between the two jets is the same (as visible in terms of intensity in our OES measurements), argon metastables contribute to the degradation of the dye via subsequent reactions at the interface or in the gas phase.<sup>14,43</sup> The argon metastable state density ( $1s_5$ ) can

reach levels of  $10^{14} \text{ cm}^{-3}$  depending on the applied voltage and gas composition.<sup>46</sup>

The treated samples, using the argon plasma jet, were noticeably cold to human touch while the samples treated with the helium plasma jet were warm. A measurement of the helium samples with a thermocouple yielded a temperature of  $50^\circ\text{C}$  while argon samples were around  $30^\circ\text{C}$ . Previous research found an increase in MB degradation with higher gas temperature, but that does not occur in our work.<sup>47</sup> Because heat is dissipated into the solution with the helium plasma jet, the input power is not used as effectively as by the argon plasma jet. To compare the efficiency of the plasma jets quantitatively, the energy yield was calculated using the standard formula,

$$\text{Energy Yield} = \frac{V \times C_0 \times \text{Degradation \%} \times \frac{1}{100}}{P \times t}, \quad (9)$$

where  $V$  is the solution volume,  $C_0$  is the initial concentration,  $P$  is the power, and  $t$  is the time. After 15 min, the energy yield was  $0.19 \text{ g kW}^{-1} \text{ h}^{-1}$  at 40% for helium while it was  $0.34 \text{ g kW}^{-1} \text{ h}^{-1}$  at 82% for argon.

#### IV. CONCLUSION

In conclusion, we have presented a comparison of the effectiveness of two plasma jets, helium and argon, operating under the same conditions on MB degradation. The atomic oxygen is contained within different states: the  $O(^1S)$  at 557.7 nm for the argon plasma jet and non-metastable states for the helium plasma jet (777 and 844 nm). The argon plasma jet degrades the dye to a clear solution faster than the helium plasma jet and is more energy efficient. Based on our OES measurements and previous modeling, we have provided an understanding of the reactions to produce the

reactive species responsible for MB degradation. We have shown here that oxygen and metastable argon are as important to MB degradation as OH and other established reactive species. The argon plasma jet is better suited for MB degradation because it produces more O, which is the basis for producing subsequent reactive species. Some species such as singlet delta oxygen,  $O_2(a^1\Delta_g)$ , are unlikely to be present without additional  $O_2$  gas,<sup>48</sup> while ozone is unlikely to be important unless specifically generated. The  $O(^1S)$  is a very useful state of atomic oxygen,<sup>22</sup> and the argon plasma jet in our experiment produces significant amounts of this reactive species (a maximum of  $\sim 10^{16} \text{ cm}^{-3}$ ).<sup>20</sup> The low cost of argon compared to helium ( $\sim 2.5$  times cheaper) and the significant amounts of oxygen produced by the argon plasma jet are important reasons to consider the APPJ system we have presented here for MB degradation. Future research will focus on optimizing the current system and scaling up the treatment process.

## ACKNOWLEDGMENTS

This work was supported with funding from the NSF EPSCoR Program, under Grant No. OIA-1655280. S.J. and E.M.A. thank Auburn University and Professor Edward Thomas, Jr., for providing the research infrastructure. S.J. and E.M.A. thank G. Veda Prakash for useful discussions concerning the experimental design and data analysis.

## DATA AVAILABILITY

The data that support the findings of this study are available from the corresponding author upon reasonable request.

## REFERENCES

- 1 J. Winter, R. Brandenburg, and K.-D. Weltmann, *Plasma Sources Sci. Technol.* **24**, 064001 (2015).
- 2 M. Keidar, D. Yan, I. I. Beilis, B. Trink, and J. H. Sherman, *Trends Biotechnol.* **36**, 586 (2017).
- 3 X. Lu, G. V. Naidis, M. Laroussi, and K. Ostrikov, *Phys. Rep.* **540**, 123 (2014).
- 4 E. Klimiuk, K. Kabardo, Z. Gusiatin, and U. Filipkowska, *Pol. J. Environ. Stud.* **14**, 771 (2005).
- 5 Y. C. Wong, Y. S. Szeto, W. H. Cheung, and G. McKay, *J. Appl. Polym. Sci.* **92**, 1633 (2004).
- 6 T. Robinson, G. McMullan, R. Marchant, and P. Nigam, *Bioresour. Technol.* **77**, 247 (2001).
- 7 E. Roufegari-Nejhad, M. Sirousazar, V. Abbasi-Chiyaneh, and F. Kheiri, *J. Polym. Environ.* **27**, 2239 (2019).
- 8 S. A. Umoren, U. J. Etim, and A. U. Israel, *J. Mater. Environ. Sci.* **4**, 75 (2013).
- 9 A. Fahmy, A. El-Zomrawy, A. M. Saeed, A. Z. Sayed, M. A. Ezz El-Arab, H. Shehata, and J. Friedrich, *Plasma Res. Express* **2**, 015009 (2020).
- 10 M. Magureanu, D. Piroi, F. Gherendi, N. B. Mandache, and V. Parvulescu, *Plasma Chem. Plasma Process.* **28**, 677 (2008).
- 11 M. Magureanu, N. B. Mandache, and V. I. Parvulescu, *Plasma Chem. Plasma Process.* **27**, 589 (2007).
- 12 L. Wu, Q. Xie, Y. Lv, Z. Wu, X. Liang, M. Lu, and Y. Nie, *Water* **11**, 1818 (2019).
- 13 H. Aoki, K. Kitano, and S. Hamaguchi, *Plasma Sources Sci. Technol.* **17**, 025006 (2008).
- 14 M. C. García, M. Mora, D. Esquivel, J. E. Foster, A. Rodero, C. Jiménez-Sanchidrián, and F. J. Romero-Salguero, *Chemosphere* **180**, 239 (2017).
- 15 E. Abdel-Fattah, *J. Electroanal. Chem.* **101**, 103360 (2019).
- 16 F. Huang, L. Chen, H. Wang, and Z. Yan, *Chem. Eng. J.* **162**, 250 (2010).
- 17 W. Van Gaens and A. Bogaerts, *J. Phys. D: Appl. Phys.* **46**, 275201 (2013).
- 18 R. Bussiahn, E. Kindel, H. Lange, and K.-D. Weltmann, *J. Phys. D: Appl. Phys.* **43**, 165201 (2010).
- 19 A. Schmidt-Bleker, J. Winter, A. Bösel, S. Reuter, and K.-D. Weltmann, *Plasma Sources Sci. Technol.* **25**, 015005 (2016).
- 20 S. Jaiswal, E. M. Aguirre, and G. V. Prakash, *Sci. Rep.* **11**, 1893 (2021).
- 21 A.-M. Pointu, A. Ricard, B. Dodet, E. Odic, J. Larbre, and M. Ganciu, *J. Phys. D: Appl. Phys.* **38**, 1905 (2005).
- 22 E. V. Shun'ko and V. S. Belkin, *J. Appl. Phys.* **102**, 083304 (2007).
- 23 D. E. Ashpis, M. C. Laun, and E. L. Griebeler, Technical Report NASA/TM-2012-0217449, National Aeronautics and Space Administration, 2012.
- 24 R. R. Khanikar, P. J. Boruah, and H. Bailung, *Plasma Res. Express* **2**, 045002 (2020).
- 25 W. Olchawa, R. Olchawa, and B. Grabowski, *Eur. Phys. J. D* **28**, 119 (2004).
- 26 N. Balcon, A. Aanesland, and R. Boswell, *Plasma Sources Sci. Technol.* **16**, 217 (2007).
- 27 I. Jögi, R. Talviste, J. Raud, K. Piip, and P. Paris, *J. Phys. D: Appl. Phys.* **47**, 415202 (2014).
- 28 R. F. Boivin, "Study of the different line broadening mechanisms for the laser induced fluorescence diagnostic of the HELIX and LEIA plasmas," Technical Report PLP-039, West Virginia University, 1998.
- 29 E. E. Whiting, *J. Quant. Spectrosc. Radiat. Transfer* **8**, 1379 (1968).
- 30 A. Y. Nikiforov, C. Leys, M. A. Gonzalez, and J. L. Walsh, *Plasma Sources Sci. Technol.* **24**, 034001 (2015).
- 31 A. Kramida, Y. Ralchenko, J. Reader, and NIST ASD Team, NIST Atomic Spectra Database, ver. 5.7.1, 2019.
- 32 V. Léveillé and S. Coulombe, *Plasma Processes Polym.* **3**, 587 (2006).
- 33 S. H. Pandya and K. N. Joshipura, *J. Geophys. Res.: Space Phys.* **119**, 2263, <https://doi.org/10.1002/2013ja019208> (2014).
- 34 R. Xiong, A. Nikiforov, P. Vanraes, and C. Leys, *J. Adv. Oxid. Technol.* **15**, 197 (2012).
- 35 P. Reddy, B. Raju, J. Karupiah, E. Reddy, and C. Subrahmanyam, *Chem. Eng. J.* **217**, 41 (2013).
- 36 T. Maehara, H. Toyota, M. Kuramoto, A. Iwamae, A. Tadokoro, S. Mukasa, H. Yamashita, A. Kawashima, and S. Nomura, *Jpn. J. Appl. Phys., Part 1* **45**, 8864 (2006).
- 37 X.-J. Shao, N. Jiang, G.-J. Zhang, and Z. Cao, *Appl. Phys. Lett.* **101**, 253509 (2012).
- 38 Y. S. Seo, A. H. Mohamed, K. C. Woo, H. W. Lee, J. K. Lee, and K. T. Kim, *IEEE Trans. Plasma Sci.* **38**, 2954 (2010).
- 39 T. B. Petrova, D. R. Boris, M. Hinshelwood, M. J. Johnson, E. D. Gillman, and S. G. Walton, *Phys. Plasmas* **27**, 103512 (2020).
- 40 X. L. Deng, A. Yu. Nikiforov, P. Vanraes, and Ch. Leys, *J. Appl. Phys.* **113**, 023305 (2013).
- 41 Y. Sun, Y. Liu, R. Li, G. Xue, and S. Ognier, *Chemosphere* **155**, 243 (2016).
- 42 P. Attri et al., *Sci. Rep.* **6**, 34419 (2016).
- 43 L. Chandana, P. M. K. Reddy, and C. Subrahmanyam, *Chem. Eng. J.* **282**, 116–122 (2015).
- 44 A. Corney and O. M. Williams, *J. Phys. B: At. Mol. Phys.* **5**, 686 (1972).
- 45 R. A. Young, G. Black, and T. G. Slinger, *J. Chem. Phys.* **49**, 4758 (1968).
- 46 E. Es-sebbar, G. Bauville, M. Fleury, S. Pasquiers, and J. S. Sousa, *J. Appl. Phys.* **126**, 073302 (2019).
- 47 I. Miyamoto, T. Maehara, H. Miyaoka, S. Onishi, S. Mukasa, H. Toyota, M. Kuramoto, S. Nomura, and A. Kawashima, *J. Plasma Fusion Res.* **8**, 627 (2009).
- 48 Y. Inoue and R. Ono, *J. Phys. D: Appl. Phys.* **50**, 214001 (2017).